Stable water isotope monitoring network of different water bodies in Shiyang River Basin, a typical arid river in China

Guofeng Zhu[a,b,*], Yuwei Liu[a,b], Peiji Shi[a,b], Wenxiong Jia[a,b], Junju Zhou[a,b], Yuanfeng Liu[a,b], Xinggang Ma[a,b], Hanxiong Pan[a,b], Yu Zhang[a,b], Zhiyuan Zhang[a,b], Zhigang Sun[a,b], Leilei Yong[a,b], Kailiang Zhao[a,b]

[a] College of Geography and Environment Science, Northwest Normal University, Lanzhou 730070, Gansu, China
[b] Shiyang River Ecological Environment Observation Station, Northwest Normal University, Lanzhou 730070, Gansu, China

Correspondence to: Guofeng Zhu (zhugf@nwnu.edu.cn)

Abstract. Ecosystems in arid areas are fragile and are easily disturbed by various natural and human factors. As natural tracers widely exist in nature, stable isotopes can be valuable for studying environmental change and the water cycle. From 2015 to 2020, we took the Shiyang River Basin, which has the highest utilization rate of water resources and the most prominent contradiction of water use, as a typical demonstration basin to establish and improve the isotope hydrology observation system. The data in the observation system are classified by water type (precipitation, river water, lake water, groundwater, soil water, and plant water). Six observation systems with stable isotopes as the main observation elements, including river source region, oasis region, reservoir channel system region, oasis farmland region, ecological engineering construction region, and salinization process region, have been built, and meteorological and hydrological data have also been collected. We will gradually improve the various observation systems, increase the data of observation sites, and update the data set yearly. We can use these data to research the continental river basin ecological hydrology, such as surface water evaporation loss, landscape river water cycle impact of the dam, dam water retention time, oasis farmland irrigation methods, and the atmosphere, such as circulation water inland contribution to inland river precipitation, climate transformation, below-cloud evaporation effect, extreme climate events, which provides a scientific basis for water resources utilization and ecological environment restoration in the arid area. The datasets are available at https://data.mendeley.com/datasets/vhm44t74sy/1 (Zhu, 2022).

Keywords. Stable isotopes; Monitoring network; Shiyang River Basin; Arid river

1 Introduction

Arid areas account for 33% of the world's total land area and are characterized by a lack of water vapor sources and fragile ecosystems, which are easily disturbed by various natural and human factors (Qin and Thomas, 2014;

Arheimer et al., 2017; Alam et al., 2019). Global and regional climate change exacerbate the uncertainty of water resources (Chen et al., 2017; Thompson et al., 2000; Zhang et al., 2021). In addition, under the influence of human activities, rivers' hydrological and ecological processes in arid areas, especially in the middle and lower reaches, have

30 changed, resulting in many ecological and environmental problems (Gibson et al., 2016; Grill et al., 2015; Shah et al., 2021). To clarify the eco-hydrological process of the arid inland river basin is of great significance to other arid regions in the world.

Although stable isotopes such as δ^2H and $\delta^{18}O$ account for a small proportion in natural water bodies, they respond quickly to historical records of environmental changes and water cycle evolution (Vandenschrick et al., 2002;

35 Hah et al., 2020). Stable isotopes provide a useful means of studying regional and global water cycles (Craig, 1961; Vallet-Coulomb et al., 2008; Bowen et al., 2012; Gibson et al., 2016). However, isotopic fractionation runs through every link of the water cycle (Song et al., 2017; Dansgaard, 1964). The hydrogen and oxygen isotopic compositions of different water bodies are influenced by isotopic fractionation (Gu, 1995; Risi et al., 2010a; Sun et al., 2012; Min et al., 2018). At the same time, isotope fractionation may occur in hydrogen and oxygen isotope experiments. For example,

40 the physical and chemical properties of soil may lead to the fractionation of hydrogen and oxygen in soil water (Meissner et al., 2014). In addition, incomplete extraction of water during cryogenic distillation may lead to isotope fractionation (Orlowski et al., 2016). We have always known the existence of these "problems", but compared with traditional hydrological methods, the high accuracy of isotope measurement technology and its resistance to external factors have made it widely used in the fields of hydrology, water resources, and the water cycle, and become an

45 effective tool for solving many major scientific problems (Gat et al., 1996; Kralik et al., 2004; Li and Garzione, 2017). In particular, precipitation-surface water-soil water-groundwater can be regarded as a unified "system" to quantitatively study the hydraulic connection between different water bodies (Burns et al., 1998; Gudkov et al., 2021; Zannoni et al., 2019). Due to the limitations of sampling time, sampling space, and the experimental analysis, there has been a lack of comprehensive research on different water bodies in the same area over a long time, which makes it challenging to

50 study the water cycle in a specific area by using stable isotope comparison.

There are many rivers and watersheds similar to the Shiyang River basin in the world. Angerman River, located in northern Sweden, is the third largest river in Sweden, with a total length of 450 km and a watershed area of 32,000 km^2 (Mitrovica and Forte, 2004). Many hydropower stations are built along the Angerman River due to the rapids (Melin, 1970). Glomma River is the longest river in Norway. 13% of Norway's land area belongs to the Glomma River, with a

55 total length of 598 km and a watershed area of 42,000 km^2 (Petterson et al., 2016). The agricultural area accounts for 5.8% of the catchment area, and the catchment area has about 675,000 residents (Helland, 2001). Digul River' in Indonesia, with a total length of 525 km, covers an area of 29,700 km^2 and is covered with swamps and rainforests (Ploeg, 2013). Compared with the Shiyang River basin, these rivers and basins have little difference in basin area (the Shiyang River basin covers 41,600 km^2) but significant difference in length (the Shiyang River is 250 km). The

60 Shiyang River has a short length, a large basin area, and a large population, which makes the Shiyang River basin one of the inland river basins with high population density in the world. Its per capita water resources are low, with a net utilization rate of over 95%, far exceeding the internationally recognized reasonable utilization rate (Wei et al., 2013; Li et al., 2013). Compared with the Glomma river, the Shiyang basin has a large agricultural area and a dense population, but its length is short, and its development time is early, so the contradiction between water resources and

65 the ecological environment in the Shiyang river basin is the most prominent. Compared with the catchment area, the relatively short river, such as the Orinoco River in South America, has a length of 2740 km and a drainage area of 948,000 km^2 (Lavelle et al., 2013). Its drainage area is similar to that of the Yangtze River, the longest river in Asia (with a drainage area of about 1 million km2), but its length is short (the length of the Yangtze River is 4504 km)(Wang et al., 2012). The Yangtze River and Orinoco River in South America are rich in precipitation and water

70 resources, while the Shiyang River lies deep in the hinterland of Asia and Europe, with little and irregular precipitation, large evaporation, and long drought period, so the Shiyang River basin has become the focus of public attention.

We have established an isotope hydrology observation system in the Shiyang River basin, collected stable water isotope data and meteorological and hydrological data from 2015 to 2020, and compiled them into a data set. We used the data to study: (1) The contribution of circulating water to precipitation. Our research shows that plants'

evapotranspiration water vapor contribution is always greater than the surface evaporative water vapor, and different landscapes and special underlying surfaces are important factors affecting the difference in water vapor contribution (Zhu et al., 2018). (2) Below-cloud evaporation of stable precipitation isotopes in mountainous areas, oases, and deserts in arid regions. Our study shows that the below-cloud evaporation is the strongest in summer and the weakest in spring, and the humidification of the reservoir will weaken the below-cloud evaporation (Zhu et al., 2021b). (3) Evaporative losses of surface water were identified using stable isotopes. Our research shows that evaporation from surface water increases gradually from mountains to deserts, and increases in reservoir and irrigation water can lead to evaporation (Sun et al., 2021). (4) Impact of landscape dams on river water circulation in urban and rural areas. Our research shows that the cumulative effect of multiple landscape dams leads to severe water shortages in arid regions (Zhu et al., 2021a). (5) The infiltration process of oasis farmland irrigation water and its enlightenment to optimizing irrigation methods. Our study shows that irrigation water, as the primary source of recharge in this study, can reach soil layers below 1 m, effectively replacing old water in farmland soil (Zhu et al., 2021c). (6) Effects of plastic film on soil water migration in arid oasis farmland. Our research shows that mulching can effectively reduce the evaporative loss of topsoil water and improve water use efficiency during the whole maize growing season (Zhu et al., 2021d). Our work will help clarify the impact of the local water cycle and human activities on agricultural production in the Shiyang River Basin, analyze the development trend of inland river basins under global climate change, promote ecological restoration, and provide some scientific reference for the eco-hydrological research in other arid areas.

2 Study area

The Shiyang River Basin (36°29'N-39°27'N, 101°41'E-104°16'E) is located in the eastern Qilian Mountain and Hexi Corridor. The topography of the Shiyang River Basin slopes sharply from southwest to northeast, with Qilian Mountains in the south, alluvial plains and Gobi in the middle, and flood plains and deserts in the north (Zhu et al., 2020). The river is about 250 km long and covers an area of 4.16×10^4 km^2 (Wang and Gao, 2021). There are five hydrological stations in the Shiyang River Basin, Miscellaneous Wood Temple, Jiu Tiaoling, Cai Qiqiao, Nanying Reservoir, and Huanyang River

Reservoir, with average annual flows of 7.33 m³s⁻¹, 10.07 m³s⁻¹, 9.15 m³s⁻¹, 3.92 m³s⁻¹, and 3.86 m³s⁻¹, respectively. From south to north, the Shiyang River Basin covers three different climatic regions: the southern Qilian Mountain area has an snow climate with dry winter, with an annual average temperature below 6℃ and precipitation of 300-600 mm; the central corridor plain has a arid steppe climate, the annual average temperature is between 6-8℃, and the precipitation is 150-300 mm; the north has a arid desert climate, with an annual average temperature higher than 8℃ and precipitation less than 150mm (Zhu et al., 2021a; Kottek et al., 2006). The precipitation in the Shiyang River Basin is mainly concentrated in summer (71.54 mm), with the least precipitation in winter (4.22 mm); the average evaporation in summer (713.45 mm) is the largest, while the average evaporation in winter (164.4 mm) is the smallest (Appendix C Figure. C1). The irrigation system for surface water and groundwater is complete in the Shiyang River Basin, with irrigated 4.6 million hectares of cultivated land.

3 Observation network design

From 2015 to 2020, we set up 16 meteorological observation stations, 53 hydrological observation stations, 19 soil and vegetation observation stations, and 20 mu of experimental observation plots in the Datan Township. For the convenience of data recording, each monitoring point is recorded in short form. Appendix B Table. A1 presents the complete names, abbreviations, and corresponding meteorological parameters of each sampling point so that readers can match the data set. 6756 samples were collected, including 1206 precipitation samples, 1101 surface water samples, 161 groundwater samples, 3779 soil water samples, and 509 plant water samples. Figure 1 shows the distribution of six observation systems: river source region, oasis region, reservoir channel system region, oasis farmland region, ecological engineering construction region, and salinization process region. Based on the isotope data, we have carried out the following studies: studied the evaporation and the water vapor cycle in the Shiyang River Basin (Zhu et al., 2018), analyzed the runoff source and material transport in the runoff producing area of the arid area (Zhou et al., 2020; Ma et al., 2019), so as to clarify the sources of atmospheric and surface water; analyzed the influence of reservoir on the water cycle and studied the influence of ecological water transfer project on the water cycle (Zhu et al., 2021a), so as to clarify the influence of reservoir and ecological water transfer on the hydrological process, and quantify the influence of climate change and human activities on hydrology and

water resources of the basin.
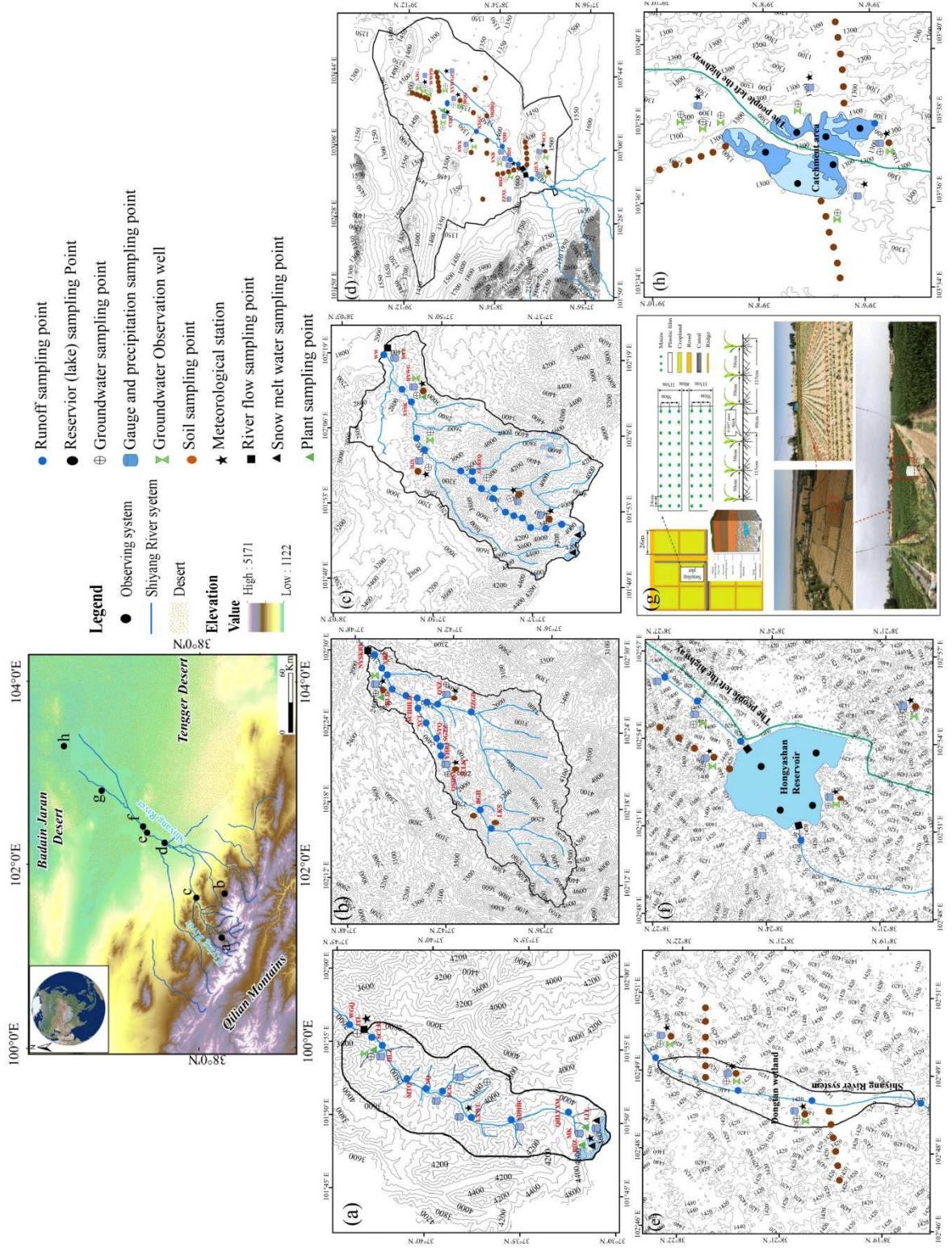
Legend

Observing system

- ● Runoff sampling point
- ● Reservior (lake) sampling Point
- ⊕ Groundwater sampling point
- ▦ Gauge and precipitation sampling point
- ⊕ Groundwater Observation well
- ● Soil sampling point
- ★ Meteorological station
- ■ River flow sampling point
- ▲ Snow melt water sampling point
- ▲ Plant sampling point

Shiyang River syetem

Desert

Elevation

Value

High : 5171

Low : 1122

4 Data and Methods

4.1 Sample collection

4.1.1 Collection of precipitation

We use standard rain gauges to collect precipitation (Appendix C Figure. C2). The rain gauge is placed in an open outdoor area and consists of rain gear, funnel, water bottle, and rain cup. The diameter of the rain gear is 20 cm, and the port of the device is horizontal. The height of the rain opening of the instrument is set to be 70 cm above the ground level. We placed an anti-evaporation polythene ball at the funnel mouth and added a layer of paraffin oil to the bottom of the container to prevent isotope fractionation caused by evaporation. After each precipitation event, we immediately transfer the collected liquid precipitation to a 100 mL high-density sample bottle. For solid precipitation, we transfer it to a high-density polyethylene sample bottle after the solid precipitation becomes liquid water at room temperature (23°C). We use Parafilm to seal the plastic bottle and at the same time affix a label with the date of collection, the type of precipitation (rain, snow, hail), and the amount of precipitation on the bottle. We stored the collected samples in a freezer at a temperature of about 4°C for experimental testing.

4.1.2 Collection of surface water and groundwater

We collect surface water (river water, lake water, reservoir water) in polyethylene bottles. We stratified samples at different depths (surface, middle, and bottom). We collected groundwater samples from groundwater monitoring wells of the Shiyang River Basin Administration Bureau, China Hydrology Bureau, and Gansu Hydrology Bureau. We seal polythene bottles with sealing film and label them with the date of sampling, depth of sampling, condition of tributaries, and mainstream.

4.1.3 Collection of soil and plant water

We collected soil at a depth of 100 cm and collected soil samples every 10 cm. The upper reaches of the Shiyang River Basin are dominated by clay, while the middle and lower reaches are dominated by clay and sandy soil. Table 1 shows the soil characteristics of farmland areas in the Shiyang River Basin. We divided the soil sample into two parts, one part into 50 mL glass bottles. The other samples were placed in 50 mL aluminum boxes, and soil water content was measured by the drying method since 2019.

Table 1 Basic information of soil samples in DTX (Zhu et al., 2021b)

Soil depth (cm)	Clay (%)	Silt (%)	Sand (%)	Soil bulk density (g/cm^3)
0-10	10.20	38.85	50.95	1.05
10-20	12.94	37.76	49.30	1.19
20-30	10.33	44.23	45.44	1.30
30-40	13.48	38.69	47.83	1.18
40-50	12.01	35.09	52.90	1.14
50-60	11.21	42.83	45.96	1.21
60-70	10.34	42.98	46.68	1.21
70-80	11.09	38.96	49.95	1.11
80-90	11.75	37.72	50.53	1.20
90-100	7.21	35.97	56.82	1.27

For trees and shrubs, we collect stems, and for herbs, we collect non-green parts at the junction of rhizomes. When sampling, we use scissors to collect vegetation stems, peel off the bark, put them in 50 mL glass bottles, and freeze them until experimental analysis. Table 2 shows the plant information.

Table 2 Basic information of plant samples

Sampling points	Vegetation types	Sample size
BDZ	Agropyron cristatum	30g ±0.5
CQQ	Corn (stem), reed, jujube (Branches), dryland willow (Branches)	30g-100g
DT	Reed	30g±0.5
DTX	Spring wheat (stem), corn (root, stem)	30g±0.5
HJX	Willow (Branches)	100g±0.5
HLD	Qinghai Spruce (Branches)	100g±0.5
HLZ	Qinghai Spruce (Branches)	100g±0.5
WWPD	Corn (stem), wheat (stem)	30g±0.5
XYWG	Poplar (Branches), wheat	100g±0.5
YXB	Corn (stem)	30g±0.5
SWX	Corn, wheat (stem)	30g±0.5
LLL	Salsola purpurea	30g±0.5

4.1.4 Collection of meteorological data

The local meteorological data were obtained by the automatic weather stations (watchdog 2000 series weather stations) erected near the sample plot. Meteorological data include temperature (℃), relative humidity (%), atmospheric pressure (hPa), dew point temperature (℃), and precipitation (mm).

4.2 Data quality

For meteorological and hydrological data, we use Manner-Kendall to test, eliminate outliers and use interpolation to fill in the missing values. We use LWIA post analysis to detect the original isotope data. LWIA software can automatically check the instrument's fault prompts and provide a batch of optional data filtering methods. Through LWIA, we can know which original data values of samples are wrong and need to be tested again and see the cause of the data error. At the same time, we will also use SPSS software to check the normality of the obtained isotope data. At present, the impact on data quality mainly comes from the following aspects:

4.2.1 Sample collection

170   When collecting precipitation samples, the precipitation was not transferred to the high-density sample bottle immediately, resulting in the enrichment of δ^2H and $\delta^{18}O$.

For vegetation samples,   the error is mainly from the samples' collection process. If the sampling time is too long, the contact time between vegetation and air becomes longer, which causes evaporation of vegetation water.

For soil samples, the error is that we collected soil samples that contained many microorganisms. The influence of

175   soil microbial activities on the results of extracted water isotopes is poorly understood. When isotope values are measured by isotope mass spectrometry, the increased CO_2 concentration released during bacterial growth leads to further errors.

4.2. 2 Experiment

The experimental(Appendix A) error is mainly because we set the same water extraction parameters for samples

180   with different soil characteristics. It is difficult to make post-mortem corrections for soil properties or the effects of extraction conditions because such information is rarely reported, and massive variability in method details is common (Walker et al., 1994). In addition, there are still measurement uncertainties in the process of water extraction, which also come from the loss of water vapor and the non-temperature heating temperature during the vacuum of the extraction system.

185   We only consider methanol and ethanol pollution in the calibration of plant sample data, but the plant and soil water extracts may contain various other pollutants. In addition, studies have shown that the mismatch between xylem and plant water sources is due to the fractionation of isotopes in the process of water absorption (Poca et al., 2019), which questioned the fact that plants did not undergo fractionation during the process of water absorption (Porporato, 2001; Meissne et al., 2014) this traditional view. However, there is no better solution, so we still use traditional

190   methods to collect samples and conduct experiments.

4.3   Data set

4.3.1 Meteorological and hydrological data set

We obtained the meteorological data includes temperature (℃), relative humidity (%), air pressure (hPa), dew point temperature (℃), and precipitation (mm). We store the obtained weather data in the corresponding weather station file. The obtained hydrological data includes annual runoff (m³/s), daily average flow (m³/s), daily average water level (m), and the inflow of Qingtu Lake and its change.

4.3.2 Stable water isotope data set

Firstly, we conducted field sampling to obtain samples of different water bodies. According to the samples' types, the samples can be divided into two categories: precipitation, river water, lake water, and groundwater can be directly tested after filtration, while soil samples and vegetation samples need to be vacuum condensed and extracted to separate the water in soil and vegetation for testing and analysis. The assembly of the data set relies mainly on the monitoring data and instrument-tested data. The extraction apparatus's use is BJJL - 2200 fully automatic vacuum condensate extraction system. The analysis instrument is LWIA - 24 d liquid water isotope analyzer (Appendix C Figure. C3). We use LIMA to test the original data produced by the analyzer. If the data passes the detection of the software, it can be included in the data set. If the data does not pass the detection of the software, we need to reuse the analyzer for analysis until the data passes the detection of the software. We use M-K test to eliminate abnormal meteorological and hydrological data.The stable isotope data set and the meteorological and hydrological data set are combined into one data set (Fig. 2).
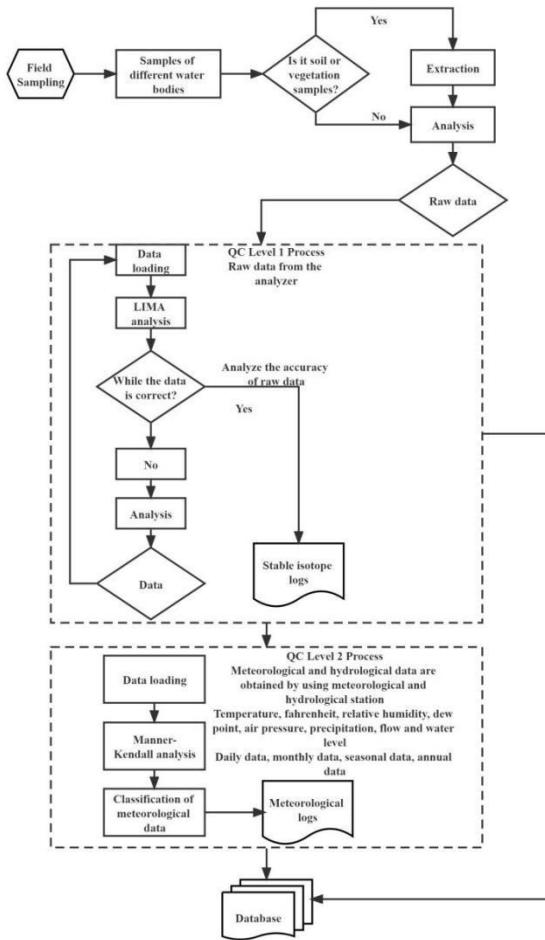
Figure. 2 Extraction, analysis of the instrument and data set production process

210 *Note:*

Database

5 Results and Discussion

5.1 Changes in runoff

Runoff is an essential part of the water cycle (Amorocho, 1968; Emori et al., 1996; Wang et al., 2009). The flow has
215 obvious seasonal changes, with a large flow in summer and a small flow in winter (Fig. 3). However, CQQ's flow
changes are more complicated. As the downstream marker station, CQQ's cross-section runoff changes directly reflect

the intensity of interference to human activities in the middle reaches. The flow of CQQ dropped sharply in June, followed by a sharp decline in April due to the agricultural water diversion for irrigation from April to June. According to Table 4, we can see that the average annual flow of JTL in the upper reaches of the Shiyang River Basin is the largest (10.07 m^3s^{-1}), while that of Huangyang River Reservoir is the smallest (3.86 m^3s^{-1}), reflecting the spatial characteristics that the average annual flow of hydrological stations in Shiyang River Basin gradually decreases from west to east and from south to north.

The annual flow dispersion coefficient can characterize the relative change trend between inter-annual changes in regional flow (Hernández-Carrasco et al., 2012). According to Table 3, we can see that the variation range of the dispersion coefficient of discharge at the five hydrological stations in the Shiyang River Basin is 0.03-0.11, indicating that the inter-annual variation of the Shiyang River is relatively large. Among them, CQQ has the largest dispersion coefficient of 0.11, which is related to the strong interference of CQQ by human activities (Liu et al., 2013; Liang et al., 2017).
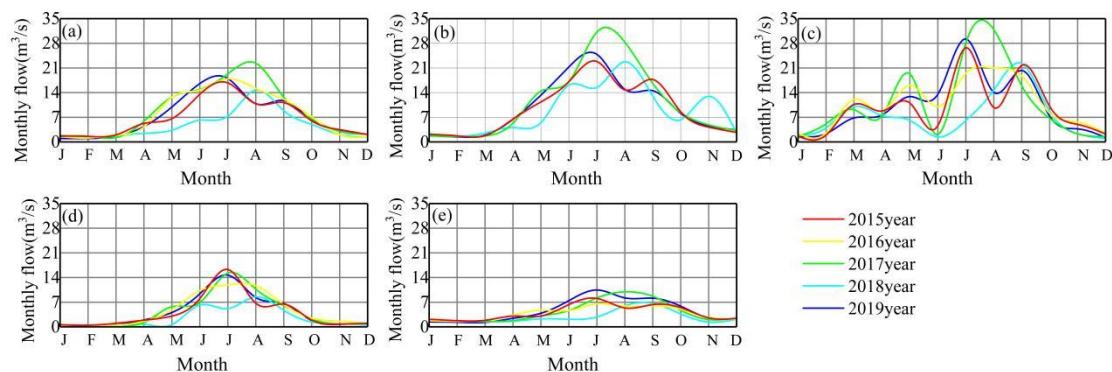
Figure. 3 Changes in the monthly average flow of five hydrological stations in the Shiyang River Basin, (a) Miscellaneous wood temple, (b) JTL, (c) CQQ, (d) Nanying Reservoir, (e) Huangyang River Reservoir

Table 3 Inter-annual variation of flow in the Shiyang River Basin

Hydrological station	Average annual flow (m^3s^{-1})	Dispersion coefficient of flow	Average annual precipitation (mm)	Annual average evaporation (mm)
Miscellaneous wood temple	7.33	0.05	351.68	1084.56
JTL	10.07	0.06	319.15	990.66

CQQ	9.15	0.11	126.82	840.75
Nanying Reservoir	3.92	0.09	242.62	1097.75
Huangyang River Reservoir	3.86	0.03	325.02	1060.55

5.2 Stable isotopes characteristics of different water bodies

In the catchment dominated by precipitation, the seasonal difference between δ^2H and $\delta^{18}O$ values is large (Anderson, 2011).The changes of δ^2H and $\delta^{18}O$ in different water bodies are roughly the same, showing good consistency and all present seasonal changes (Fig. 4). The variation of isotopes of river water, lake water, and groundwater lags behind that of precipitation, which is related to the time difference between surface runoff and underground runoff formed by precipitation. Precipitation δ^2H and $\delta^{18}O$ change in a cosine shape with time. That is, they are depleted in winter and spring and enriched in summer and autumn. This is related to the dilution of precipitation in winter and spring and strong evaporation in summer and autumn (Florea and Mcgee, 2010). Precipitation δ^2H and lake water δ^2H have large variability (the absolute value of the coefficient of variation are 0.82 and 0.7, respectively), and the precipitation $\delta^{18}O$ and plant water $\delta^{18}O$ have large variability (the absolute value of the coefficient of variation is 0.69 and 0.91, respectively). The strong evaporation of lake water in summer and the weak evaporation in other seasons make the seasonal fluctuations of lake water isotopes large. The plant water also has strong seasonal fluctuations in the isotope of plant water due to the strong transpiration in summer.
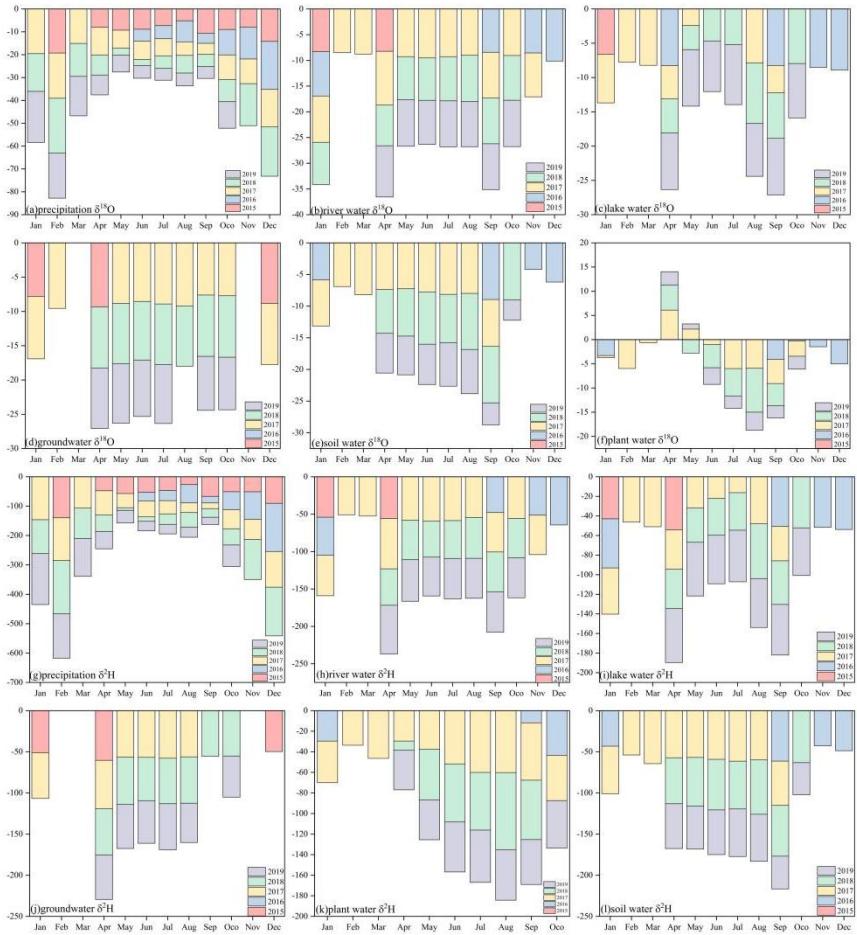
Figure. 4 Distribution of different hydrological compartments' δ²H and δ¹⁸O in the Shiyang River Basin from 2015 to 2020

5.3 Connections between different bodies of water

We used the least square method to obtain the local meteoric water line equation (LMWL): $\delta^2H=7.65\delta^{18}O + 9.75$, its slope and intercept are smaller than those of GMWL, but δ^2H and $\delta^{18}O$ maintain a good linear relationship ($R^2=0.96$), which is related to the geographical location of the study area (Fig. 5). The Shiyang River Basin is located in the Northwest inland of China, and it is subject to intense below-cloud evaporation, making the slope and intercept relatively small (Zhu et al., 2021b). It also reflects the existence of a stable isotope unbalanced fractionation effect under the arid climate background.

Precipitation, river water, lake water, groundwater, soil water, and plant water are distributed near GMWL,

indicating that they share the same water source. The deviation of the lake from GMWL indicates that it experienced

255 intense evaporation. By comparing the slope and intercept of the relation expressions δ^2H and $\delta^{18}O$ of GMWL and

different water bodies, it can be seen that, as far as the slope is concerned, precipitation is the highest (7.65), followed

by groundwater (5.11), lake water is the lowest (2.14). There is little difference between the slope of precipitation and

groundwater, which means there is a mutual recharge relationship. In terms of intercept (d), the precipitation was the

highest (d=9.75), followed by the river (d=-8.44). The light isotopes evaporate preferentially when the water body

260 evaporates in the unsaturated atmosphere (Worden et al., 2007). The combined effect of the dynamic fractionation

effect of the river accelerates the ratio of the δ^2H and $\delta^{18}O$ fractionation effects in the evaporated water vapor, resulting

in an increase in d in the water vapor and a decrease in d in the remaining water body. The average value of δ^2H and

$\delta^{18}O$ of soil water is between plant water and precipitation, but closer to precipitation (Table 4), indicating that the soil

is mainly recharged by precipitation. In the δ^2H and $\delta^{18}O$ equations of precipitation, lake water, soil water, river water,

265 plant water, and groundwater, R^2 decreases in turn, and the linear relationship between δ^2H and $\delta^{18}O$ becomes smaller

and smaller. These phenomena indicate that different water bodies have different degrees of mutual complementary.

Among them, soil water is the most miscible and is supplied by multiple water sources.

The correlation coefficient between δ^2H and $\delta^{18}O$ of lake water, groundwater, and plant water is relatively low.

The evaporation of lake water in summer is particularly intense (Salmaso and Decet, 1997), which leads to a great

270 difference in winter and summer. The stable isotopic value of lake water varies significantly in different seasons,

leading to a small correlation coefficient between them. The main recharge source of groundwater and plant water is

precipitation. It takes a certain time for precipitation to converge into surface water and groundwater, leading to

isotopic fraction, leading to a small correlation coefficient between δ^2H and $\delta^{18}O$ of the two water bodies.
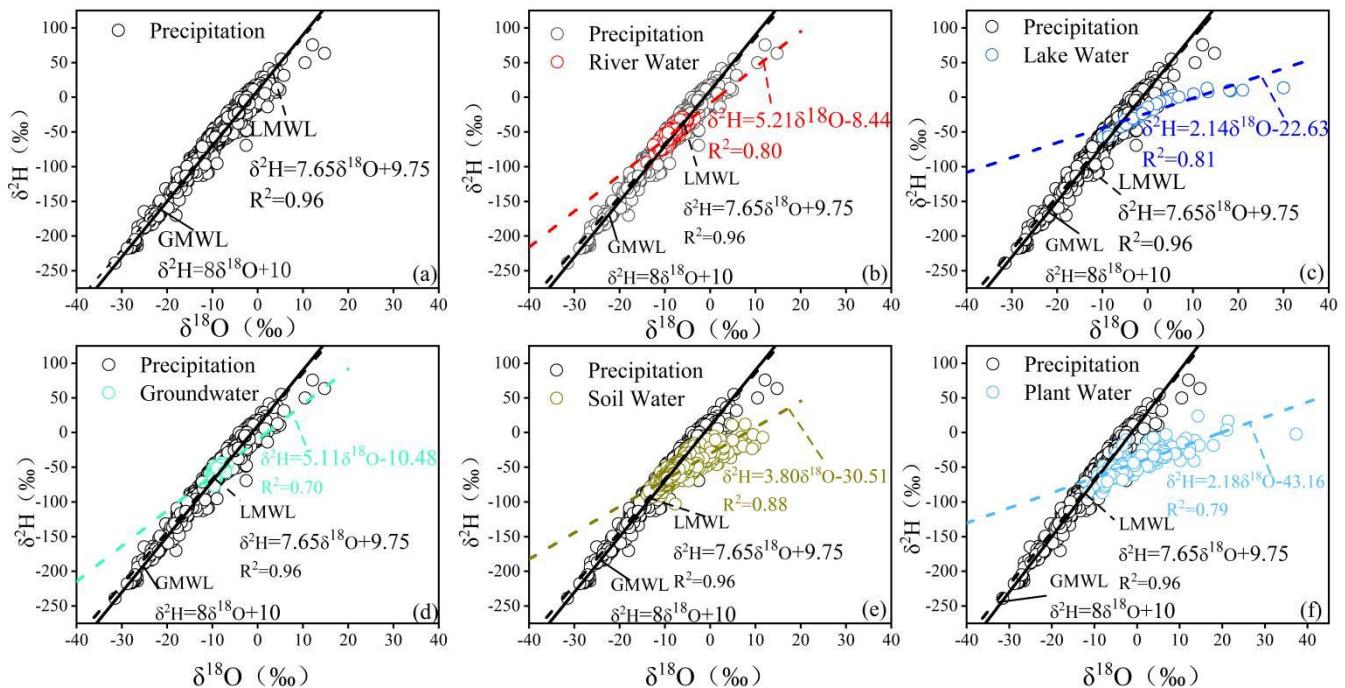
Figure. 5 The change of δ²H and δ¹⁸O in different hydrological compartments in the Shiyang River Basin, (a) is precipitation, (b) is precipitation and river water, (c) is precipitation and lake water, (d) is precipitation and groundwater, (e) is precipitation and soil water, and (f) is precipitation and plant water

Table 4 Comparison of δ²H and δ¹⁸O in different water bodies in the Shiyang River Basin

Water Type	δ²H(‰)				δ¹⁸O (‰)			
	Min	Max	Average	Coefficient of variation	Min	Max	Average	Coefficient of variation
Precipitation	-238.62	75.41	-54.63	-0.85	-31.22	14.79	-8.39	-0.71
River Water	-94.14	-28.89	-53.37	-0.12	-13.98	-3.44	-8.62	-0.11
Lake Water	-57.84	13.56	-18.43	-1.11	-9.86	30.01	1.96	4.40
Groundwater	-76.99	-43.72	-52.42	-0.10	-10.44	-6.57	-8.80	-0.08
Soil Water	-102.95	11.81	-59.39	-0.20	-13.94	11.62	-7.61	-0.37
Plant Water	-86.41	23.87	-48.15	-0.32	-11.43	37.37	-2.27	-2.54

6 Data availability

The data that support the findings of this study are openly available at https://data.mendeley.com/datasets/vhm44t74sy/1.

7 Summary and outlook

From 2015 to 2020, we took the Shiyang River Basin, which has the highest utilization rate of water resources and the most prominent contradiction of water use, as a typical demonstration basin to establish and improve the isotope hydrology observation system. We collected 6756 stable water isotope data, which were compiled into a data set along with meteorological and hydrological data. Through the analysis, we can know that: (1) The slope and intercept of LMWL in the

285 Shiyang River Basin are both smaller than GMWL, indicating that there is an obvious below-cloud evaporation effect in the Shiyang River Basin. (2) The main source of runoff recharge in the Shiyang River Basin is precipitation, and the proportion of snowmelt water and groundwater is relatively low. (3) The accumulation degree of stable isotopes in the reservoir is greater than that in other surface waters, indicating that the reservoir construction has changed the original natural evaporation pattern of the basin. This data set provides a new basis for studying the stable water isotopes of different water

290 bodies in the inland river basins.

  Due to systematic error, there are some errors in isotopic measurement results. However, the observation accuracy is affected by the operation characteristics of the instrument and the sensitivity difference of moisture to specific spectral absorption, and the observation results usually have obvious nonlinear response problems. Therefore, the data measured under the current level of technology is highly reliable. But a lot of experiments are still needed.

Appendix A

A1 Experiment analysis

A1.1 Water extraction experiment

We use vacuum condensation to extract the water from soil and plant. The extraction equipment is LI-2100 automatic vacuum condensation extraction equipment. Before water extraction, the soil and plant samples need to be taken out of the refrigerator to thaw, and each sample bottle should be stuffed with a small ball of cotton to prevent the water from evaporating. When extracting water, we set the extraction time to 150 minutes (180 minutes for plants), the temperature to 190°C, the upper limit of the vacuum pressure to 800 Pa, and the leakage rate to 0. The water evaporates from the soil or plant sample by heating it for a specified time and then freezes it in a liquid nitrogen cold trap. After the extraction, the sample is thawed at room temperature, and then we use a 1 mL syringe to extract the water sample into a labeled sample bottle, seal it and wait for the isotope experiment.

A1.2 Isotope analysis

All the water samples were analyzed in the stable isotope laboratory of Northwest Normal University using liquid water isotope analysis (DLT-100, Los Gatos Research, USA). Each water sample and isotope standard samples were injected six times in a row. To eliminate the instrument memory effect, we discarded the first two injections and used the average of the last four times as the final result. The result of the isotope measurement is expressed by the symbol "δ" and expressed in thousandths of the difference relative to the Vienna Standard Mean Ocean Water (Craig, 1961):

$$\delta_{sample}(‰) = \left[\left(\frac{R_{sample}}{R_{v\text{-}smow}} \right) - 1 \right] \times 1000 \tag{1-1}$$

In the formula, R_{sample} is the ratio of $^{18}O/^{16}O$ or $^2H/^1H$ in the collected sample, $R_{v\text{-}smow}$ is the ratio of $^{18}O/^{16}O$ or $^2H/^1H$ in the Vienna standard sample. The analytical accuracy of δ^2H and $\delta^{18}O$ are ±0.6‰ and ±0.2‰, respectively.

A2 Calibration of plant water isotope data

If the water sample contains compounds with the same wavelength absorption characteristics, it will lead to the measurement error of the laser liquid water analyzer. The most error-causing contaminants are methanol and ethanol. Therefore, we used deionized water and different concentrations of pure methanol and ethanol, combined with Los Gatos LWIA-Spectral Contamination Identifier V1.0 Spectral analysis software, to measure the pollution degree of

methanol (NB) and ethanol (BB). The δ^2H and $\delta^{18}O$ correction methods for pollution spectra were established (Brand et al., 2009; West et al., 2010). Correction results for methanol its broadband measurements of NB metric logarithmic respectively with $\Delta\delta^2H$ and $\Delta\delta^{18}O$ are significantly quadratic curve relationship, respectively is:

$$\Delta\delta^2H = 0.018(\ln NB)^3 + 0.092(\ln NB)^2 + 0.388\ln NB + 0.785 (R^2 = 0.991,\ p > 0.0001) \tag{2-1}$$

$$\Delta\delta^{18}O = 0.017(\ln NB)^3 - 0.017(\ln NB)^2 + 0.545\ln NB + 1.356 (R^2 = 0.998, p < 0.0001) \tag{2-2}$$

Its broadband measurements for ethanol correction results in BB metric and $\Delta\delta^2H$ and $\Delta\delta^{18}O$, a quadratic curve and linear relationship respectively, are:

$$\Delta\delta^2H = -85.67BB + 93.664 (R^2 = 0.747, p = 0.026)(BB < 1.2) \tag{2-3}$$

$$\Delta\delta^{18}O = -21.421BB^2 + 39.935BB - 19.089 (R^2 = 0.769,\ p < 0.012) \tag{2-4}$$

Appendix B

 Table. B1 List of basic parameters

Abbreviation	Full name	Longitude	Latitude	Elevation (m)	Average annual air temperature (℃)	Average annual precipitation (mm)	Sampling type (abbreviation)	Sampling type (full name)	Location
QHLYXM	Qinghai Forestry Project	101°51'	37°32'	3899	-	-	hs	river water	a
MK	Colliery	101°51'	37°33'	3647	-0.20	595.10	hs	precipitation	a
BDZ	Transformer Substation	101°51'	37°33'	3637	-	-	tr, zw, hs	soil, plant, river water	a
LLL	Lenglong Ling	101°28'	37°41'	3500	5.78	350.34	Js, zw	precipitation, plant water	a
SDHHC	Tunnel Junction	101°50'	37°34'	3448	-	-	hs	river water	a
LXWL	Winding Road	101°50'	37°34'	3305	-	-	hs	river water	a
NQ	Ningqian	101°49'	37°37'	3235	-	-	hs	river water	a
SCG	Ningtanhe Middle East branch mixed water	101°50'	37°38'	3068	-	-	hs, js, tr	river water, precipitation, soil	a
MTQ	Wood Bridge	101°53'	37°41'	2741	-	-	hs	river water	a
HLZ	Ranger Stations	101°53'	37°41'	2721	3.24	469.44	hs, js, tr, zw, dxs	river water, precipitation, soil, plant, groundwater	a
SCLK	Three-way Intersection	101°55'	37°43'	2590	-	-	hs	river water	a
JTL	Nine Ridge	102°02'	37°51'	2267	-	-	dxs	groundwater	a
WGQ	The Bridge of the Cultural Revolution	102°07'	37°53'	2174	-	-	hs	river water	a
BGH	Binggou River	102°17'	37°40'	2872	5.28	-	hs, tr	river water, soil	b
LKS	Two Pine	102°17'	37°40'	2832	5.69	-	hs, tr	river water, soil	b
QSHSY	Spring River	102°22'	37°38'	2747	-	-	qs	spring water	b
JCLK	Intersection	102°20'	37°41'	2544	-	-	hs, tr	river water, soil	b
QXZ	Meteorological Station	102°20'	37°42	2543	3.34	510.56	js, dxs	precipitation, groundwater	b
YHRJ	A family	102°20'	37°42'	2543	-	-	hs	river water	b
SGZZ	Sigou stckade	102°23'	37°40'	2492	10.34	675.54	hs	river water	b
SYQ	Laboratory Area	102°22'	37°42'	2438	-	-	hs, tr	river water, soil	b
JZGD	Construction Site	102°25'	37°41'	2303	-	-	hs	river water	b
XCL	Small Valley	102°24'	37°43'	2267	-	-	hs	river water	b
NCHHLH	South Nancha River	102°26'	37°43'	2163	-	-	hs	river water	b
HLD	Confluence	102°26'	37°44	2146	-	-	hs, tr, zw	river water, soil, plant	b
NYSKRK	Nanying Reservoir	102°29'	37°47'	1955	7.82	330.16	hs	river water	b
XBZ	Xuebai Toen	103°01'	38°32'	1387	10.77	-	js	precipitation	b
GGKFQ	Reform and Opening Bridge	101°58'	37°46'	2590	-	-	hs	river water	c
HJX	Huajian Township	102°00'	37°50'	2390	7.65	262.64	hs, dxs, js, tr	river water, groundwater, precipitation, soil	c
XYSK	Xiying Reservoir	102°12'	37°54'	2058	-	-	hs	river water	c
XYWG	Xiying Wugou	102°10'	37°53'	2097	7.99	197.67	hs, js, tr, zw	river water, precipitation, soil, plant	c
XYZ	Xiying Town	102°26'	37°58'	1748	10.44	491.35	js	precipitation	c
WW	Wuwei	102°37'	37°53'	1581	5.23	300.14	hs	river water	c
ZZXL	Zhuaxi Xiulong	103°20'	37°18'	3556	-2.37	500.17	js	precipitation	d
QLX	Qilian Township	102°42'	38°08'	3394	5.13	300.15	js, qs	precipitation, spring water	d
BHZ	Protection Station	102°29'	38°09'	2787	-	-	dxs	groundwater	d
SCG	Shangchigou	102°25'	38°03'	2400	7.28	377.13	js, hs, dxs	precipitation, river water, groundwater	d
YXB	Yangxia Dam	102°41'	38°01'	1489	10.76	-	js, dxs, tr, zw	precipitation, groundwater, soil, plant	d
WWPD	Wuwei Basin	102°42'	38°06'	1467	-	-	js, dxs, tr, zw	precipitation, groundwater, soil, plant	d
JDT	Jiudun Beach	102°45'	38°07'	1464	10.54	-	js	precipitation	d
HSH	Hongshui River	102°45'	38°13'	1454'	-	-	hs	river water	d
CQQ	Caiqi Bridge	102°45'	38°13'	1443	5.63	300.26	dxs, hs, tr, zw	groundwater, river water, soil, plant	d
HGG	Hongqi Valley	102°50'	38°21'	1421	8.34	113.16	js, dxs	precipitation, groundwater	d
MQBQ	Minqin Dam	103°08'	39°02'	1400	8.33	113.19	tr	soil	d
XXWGZ	Xiyin Wugou Township	102°58'	38°29'	1393	-	-	dxs	groundwater	d

SWX	Suwu Township	103°05'	38°36'	1372	9.82	155.84	dxs, tr, zw, hs	groundwater, soil, plant, river water	d
XXGC	Xiaxingou Village	102°56'	38°37'	1402	-	-	hs	river water	d
XJG	Xiajiangou	102°42'	38°07'	1200	9.36	110.18	dxs	groundwater	d
DT	Dongtan	102°47'	38°16'	1434	8.90	240.05	hs,tr, zw	river water, soil, plant	e
HYSSK	Hongyashan Reservior	102°53'	38°24'	1416	7.81	100.17	hs, dxs, tr	river water, groundwater, soil	f
BDC	Beidong Township	103°02'	38°32'	1367	9.52	155.45	dxs	groundwater	g
DTX	Datan Township	103°14'	38°46'	1349	11.49	-	js, dxs, soi, zw, hs	precipitation, groundwater, soi, plant, river water	g
QTH	Qingtu Lake	103°36'	39°03'	1313	7.86	110.79	js, dxs, ls, tr	precipitation, groundwater, lake water, soil	h

Appendix C
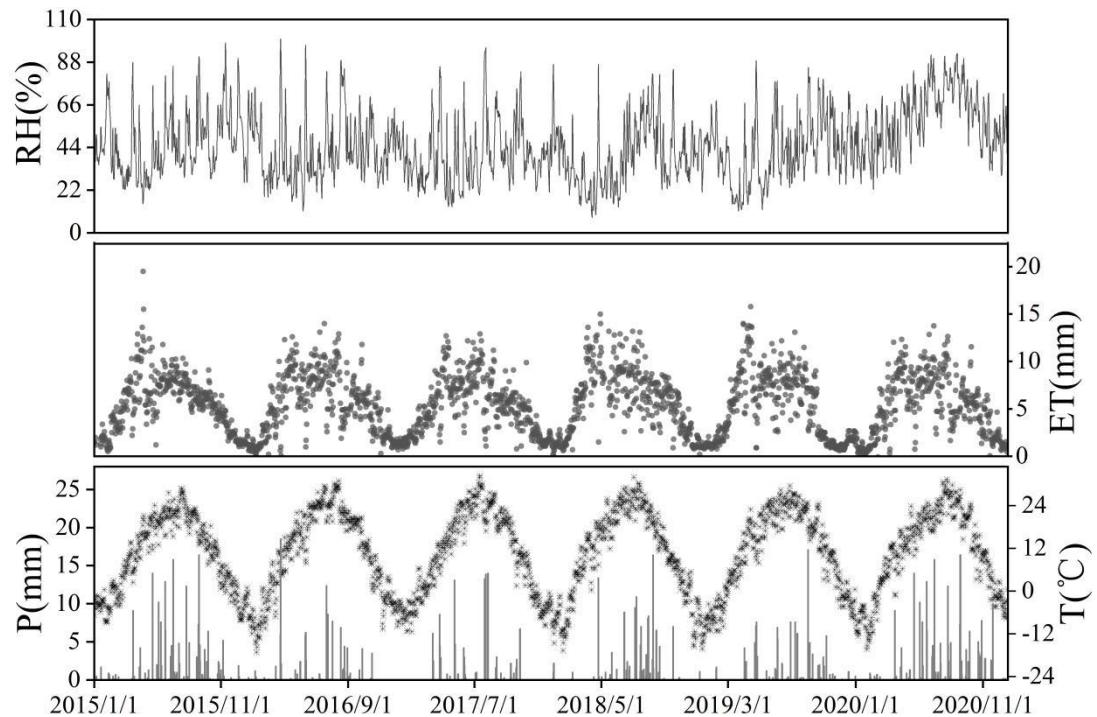
Figure. C1 Variation of meteorological parameters over time in the Shiyang River Basin, RH represents Relative Humidity, ET represents Evaporation, P represents Precipitation, and T represents Temperature

330

Figure. C2 Sampling instruments. (a) Rain gauge collecting precipitation, (b) surface water sampling, (c) sampling shears collecting vegetation stems, and (d) earth drill collecting soil samples.

335
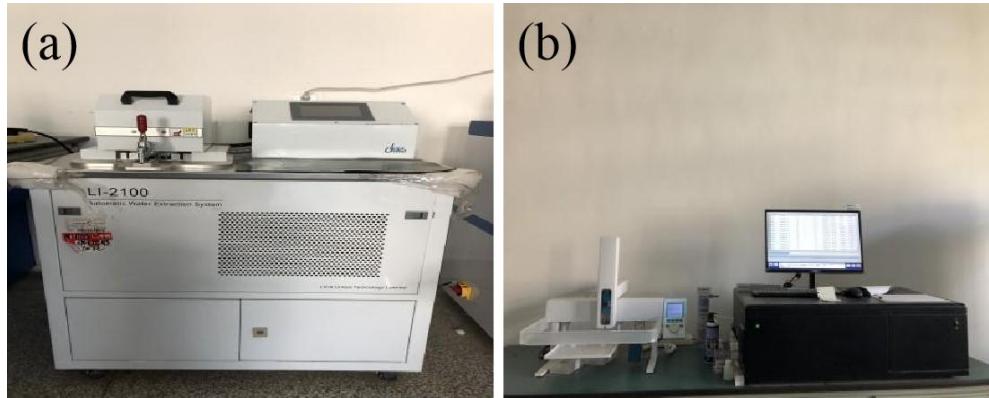
Figure. C3 Analytical instruments. (a) Li-2100 Automatic Vacuum Condensation Extraction instrument, (b) LWIA-24D Liquid water isotope Analyzer.

Author contributions

340   Guofeng Zhu and Yuwei Liu conceived the idea of the study; Guofeng Zhu, Peiji Shi, Wenxiong Jia, and Junju Zhou set up observation system; Xinggang Ma, Hanxiong Pan,Yu Zhang, Zhiyuan Zhang, and Leilei Yong were responsible for field sampling; Zhigang Sun participated in the experiment; Kailiang Zhao and Yuanfeng Liu participated in the drawing; Yuwei Liu wrote the paper. All authors discussed the results and revised the manuscript.

345 **Competing interests**

The authors declare no competing interests.

Acknowledgement

This research was financially supported by National Natural Science Foundation of China (41867030, 41971036, 41661005). The authors thank the colleagues in the Northwest Normal

350 University for their help in fieldwork, laboratory analysis, and data processing.

References

Alam, S., Gebremichael, M., Li, R., Dozier, J., and Lettenmaier, D. P.: Climate change impacts on groundwater storage in the central valley, California, Climatic. Change., 157, doi:10.1007/s10584-019-02585-5, 2019.

355 Amorocho, J.: Reply to "Discussion on Paper by Amorocho, J. ' The Nonlinear Prediction Problem in the Study of the Runoff Cycle', Water Resources Research., 4, doi: 10.1029/WR004i003p00686, 1968.

Anderson, Lesleigh.: Holocene record of precipitation seasonality from lake calcite $\delta^{18}O$ in the central Rocky Mountains, United States, Geology., 39(3): 211-214, doi: 10.1130/G31575.1, 2011.

Arheimer, B., Donnelly, C. and Lindstrom, G.: Regulation of snow-fed rivers affects flow regimes

360 more than climate change,   Nat. Commun., 8, 62, doi:10.1038/s41467-017-00092-8, 2017.

Bowen, G. J., Kennedy, C. D., Henne, P. D., and Zhang, T. L.: Footprint of recycled water subsidies downwind of Lake Michigan, Ecosphere., 3, 1–16, doi:10.1890/ES12-00062.1, 2012.

Burns, S. J., Matter, A., Frank, N., and Mangini, A.: Speleothem-based paleoclimate record from northern Oman, Geology., 26, 499–502, doi:10.1130/0091-7613(1998)0262.3.CO;2, 1998.

365 Brand, W. A., Geilmann, H., Crosson, E. R., and Rella, C. W.: Cavity ring‐down spectroscopy versus high-temperature conversion isotope ratio mass spectrometry; a case study on δ^2H and $\delta^{18}O$ of pure water samples and alcohol/water mixtures, Rapid. Commun. Mass. Sp.,   23, doi:10.1002/rcm.4083, 2009.

Chen, Y.N., Li, Z., Fang, G.H., and D, H.J.: Research on the impact of climate change on water

370 resources in Tianshan Mountains in Central Asia, Acta.   Geographica.   Sinica., 72, 9, 2017.

Craig, H.: Isotopic variation in meteoric waters, Science., 133, 1702-1703. doi:10.1126/science.133.3465.1702, 1961.

Dansgaard, W: Stable isotopes in precipitation, Tellus., 16, 436-468, doi:10.1111/j.2153-3490.1964.tb00181.x, 1964.

375   Emori, S., Abe, K., Numaguti, A., and Mitsumoto, S.: Sensitivity of a Simulated Water Cycle to a Runoff Process with Atmospheric Feedback, Journal of the Meteorological Society of Japan.,74(6):815-832, doi:10.2151/jmsj1965.74.6_815, 1996.

Florea, L. J., Mcgee, R. K.: Stable isotopic and geochemical variability within shallow groundwater beneath a hardwood hammock and surface water in an adjoining slough (Everglades National Park,
380   Florida, USA), Isotopes Environ Health Stud.,46(2):190-209, doi: 10.1080/10256016.2010.494770, 2010.

Gat, J. R.: Oxygen and hydrogen isotopes in the hydrologic cycle, Annual. Rev. Earth. Pl. Sc., 24, 255-262, doi:10.1146/ANNUREV.EARTH.24.1.225, 1996.

Gibson, J. J., Birks, S., and Yi, Y.: Stable isotope mass balance of lakes: a contemporary perspective,
385   Quaternary. Sci. Rev., 131, 316-328, doi:10.1016/j.quascirev.2015.04.013, 2016.

Gibson, J. J., Edwards, T., Birks, S. J., Amour, N., Buhay, W. M., Mceachern, P., Wolfe, B. B., and Peters, D. L.: Progress in isotope tracer hydrology in Canada, Hydrol. Processes., 19, doi:10.1002/hyp.5766, 2010.

Grill, G., Lehner, B, Lumsdon, A. E., Macdonald, G. K., Zarfl, C., and Reidy, L. C.: An index-based
390   framework for assessing patterns and trends in river fragmentation and flow regulation by global dams at multiple scales, Environ. Res. Lett., 10, doi:10.1088/1748-9326/10/1/015001, 2015.

Gu, W. Z.: Using environmental isotopes and hydrological experiments to study runoff generation methods in catchment areas, J. Hydraul. Eng., (005), 9-17,1995.

Gudkov, A. V., Tokarev, I. V., and Tolstikhin, I. N.: The formation and balance of the atmospheric
395   precipitations, surface water, and groundwater on the southern slopes of the khibiny massif (based on data on the isotopic composition of oxygen and hydrogen), Water. Resour., 48, 124-132, doi:10.1134/S0097807821010164, 2021.

Hah, A., Nmha, B., Gls, C., Yyd, E., Bw, C., and Krh, F.: Effects of seasonal and interannual variability in water isotopes (δ^2H, δ^{18}O) on estimates of water balance in a chain of seven prairie lakes -
400   sciencedirect, J. Hydrol. X., doi:10.10.1016/j.hydroa.2020.100069, 2020.

Helland, A.: The Importance of Selective Transport and Sedimentation in Trend Monitoring of Metals in Sediments. An Example from the Glomma Estuary, East Norway,Water. Air. Soil. Poll., 126, 339-361, doi: 10.1023/A:1005243728540, 2001.

Hernández-Carrasco, I., López, C., Hernández-García, E., and Turiel, A.: Seasonal and regional
405   characterization of horizontal stirring in the global ocean, Journal of Geophysical Research: Oceans.,117(C10), doi:10.1029/2012JC008222, 2012.

Kottek, M., Grieser, J., Beck, C., Rudolf, B., & Rubel, F.: World map of the Köppen-Geiger climate classification updated, Hydrol. Earth. Syst. Sc., 11(3), 259-263.doi: 10.1127/0941-2948/2006/0130, 2006.

410   Kralik, M., Papesch,W., and Stichler, W.: Austrian Network of Isotopes in Precipitation (ANIP): Quality assurance and climatological phenomenon in one of the oldest and densest networks in the world, Isotope Hydrology and Integrated, Water. Reso. Manag., 146-149, 2004.

Lavelle, P., Rodríguez, N., Arguello, O., Bernal, J., Botero, C., Chaparro, P., Gómez, Y., Gutiérrez,A., del Pilar Hurtado, M., Loaizaa, S., Pullidoc,S. X., Rodríguez, E., Sanabriaa, C., Velásquez, E., and

415 Fonte, S. J.: Soil ecosystem services and land use in the rapidly changing Orinoco River Basin of Colombia, Agr. Ecosys. Environ., 185, 106-117, doi: 10.1016/j.agee.2013.12.020, 2014.

Liang, B. B., Shi, P. J., Wang, W., Tang, X., Zhou, W. X., and Jing, Y.: Integrated assessment of ecosystem quality of arid inland river basin based on RS and GIS: A case study on Shiyang River Basin, Northwest China, The Journal of Applied Ecology., , 28(1): 199-209,
420 doi:10.13287/j.1001-9332.201701.019, 2017.

Li, L., and Garzione, C. N.: Spatial distribution and controlling factors of stable isotopes in meteoric waters on the Tibetan Plateau: implications for paleoelevation reconstruction, Earth. Planet. Sci. Lett., 460, 302-314, doi:10.1016/j.epsl.2016.11.046, 2017.

Li, Z., Li, X. Y., and Sun, J.: Impact of Climate Change on Water Resources in the Shiyang River Basin
425 and the Adaptive Measures for Energy Conservation and Emission Reduction, Applied Mechanics & Materials., 405-408:2167-2171, doi: 10.4028/www.scientific.net/AMM.405-408.2167, 2013.

Liu, H. M., Shi, P. J., Zhou, J. J., Liu, H., and Sun, H.: Characteristics and influencing factors of runoff consumption in the midstream of Shiyang river, Prog Geogr., 32:87-94. doi: 10.3724/SP.J.1033.2013.00087, 2013.

430 Ma, H.Y., Zhu, G. F., Zhang,Y., Pan, H. X., Guo, H. W., Jia, W. X., Zhou, J. J., Yong, L. L., and Wan, Q. Z.: The effects of runoff on Hydrochemistry in the Qilian Mountains: a case study of Xiying River Basin, Environ. Earth. Sci., (13), doi:10.1007/s12665-019-8384-z, 2019.

Meissner, M., Köhler, M., Schwendenmann, L., Hölscher, D., and Dyckmans, J.: Soil water uptake by trees using water stable isotopes (δ^2H and δ^{18}O) a method test regarding soil moisture, texture and
435 carbonate, Plant, Soil., 376, 327–335, doi:10.1007/s11104-013-1970-z, 2014.

Melin R.: Hydrological regions in Scandinavia and Finland, Hydrol. Res., 1(1): 5-37, doi:10.2166/nh.1970.0001, 1970.

Min, Z., Hu, Y., Cheng, Z., Liu, Z., Rui, Y., and   Bo, C.: Effects of land cover on variations in stable hydrogen and oxygen isotopes in karst groundwater: a comparative study of three karst catchments in
440 guizhou province, southwest China, J. Hydrol., 565, 374-385, doi:10.1016/j.jhydrol.2018.08.037, 2018.

Mitrovica J X, Forte A M.: A new inference of mantle viscosity based upon joint inversion of convection and glacial isostatic adjustment data, Earth. Planet. Sci. Lett., 225(1-2): 177-189, doi:10.1016/j.epsl.2004.06.005, 2004.

Orlowski, N., Breuer, L., and McDonnell, J. J.: Critical issues with cryogenic extraction of soil water
445 for stable isotope analysis. Ecohydrology., 9, 1-5, 2016.

Petterson, S. R., Stenström, T. A., and Ottoson, J.: A theoretical approach to using faecal indicator data to model norovirus concentration in surface water for QMRA: Glomma River, Norway, Water. Res., 91, 31-37, doi: 10.1016/j.watres.2015.12.037, 2016.

Ploeg, A.: Jan Pouwer's field research in the Star Mountains, west New Guinea, Oceania., 83(1), 49-56,
450 doi: 10.1002/ocea.5005, 2013.

Poca, M., Coomans, O., Urcelay, C., Zeballos, S. R , and   Boeckx, P.: Isotope fractionation during root water uptake by acacia caven is enhanced by arbuscular mycorrhizas, Plant. Soil., (3), doi:10.1007/s11104-019-04139-1, 2019.

Porporato, L.: Plants in water-controlled ecosystems: active role in hydrologic processes and response
455 to water stress, Adv. Water. Resource., 24, 725-744, doi:10.1016/S0309-1708(01)00005-7, 2001.

Qin, D. H., and Thomas, S.: Highlights of the IPCC Fifth Assessment Report by Working Group I, Progress in Climate Change Research., 1-6, 2014.

Risi, C., Bony, S., Vimeux, F., Chong, M., and Descroix, L.: Evolution of the stable water isotopic composition of the rain sampled along Sahelian squall lines, Q. J. Roy. Meteor. Soc., 136, 227-242, doi:10.1002/qj.485, 2010a.

Shah, D., Shah, H. L., Dave, H. M., and Mishra, V.: Contrasting influence of human activities on agricultural and hydrological droughts in India, Sci. Total. Environ., 774, doi:10.1016/j.scitotenv.2021.144959, 2021.

Song, C., Wang, G., Liu, G., Mao, T., Sun, X., and Chen, X.: Stable isotope variations of precipitation and streamflow reveal the young water fraction of a permafrost watershed, Hydrol. Processes., 31, 935-947, doi:10.1002/hyp.11077, 2017.

Sun, X., Chen, J., Shi, G., Tan, H., and Su, Z.: Hydrogen and oxygen isotopic variations of different water bodies in evaporation and rainfall infiltration processes, J. Agr. Eng., 28, 100-105, doi:10.3969/j.issn.1002-6819.2012.04.016, 2012.

Sun, Z.G., Zhu, G. F., Zhang, Z. X., Xu, Y. X., Yong, L. L. , Wan, Q. Z., Ma, H. Y., Sang, L. L., and Liu, Y. Y.: Identifying surface water evaporation loss of inland river basin based on evaporation enrichment model, Hydrol. Processes., 35(3), e14093, doi:10.1002/hyp.14093, 2021.

Thompson, L. G., Yao, T., Mosleythompson, E., Davis, M. E., Henderson, K. A., and Lin, P.: A high-resolution millennial record of the South Asian Monsoon from Himalayan Ice Cores, Science., 289, 1916-1920, doi:10.1126/science.289.5486.1916, 2000.

Vallet-Coulomb, C., Gasse, F., and Sonzogni, C.: Seasonal evolution of the isotopic composition of atmospheric water vapour above a tropical lake: deuterium excess and implication for water recyling, Geochimica. Et. Cosmochimica. Acta., 72, 4661–4674, doi:10.1016/j.gca.2008.06.025, 2008.

Vandenschrick, G., Wesemael, B. V., Frot, E., Pulido-Bosch, A., Molina L. b., Stiévenard, M., and Souchez, R.: Using stable isotope analysis (δD– $\delta^{18}O$) to characterise the regional hydrology of the Sierra de Gador, south east Spain, J. Hydrol., 265, 43-55, doi:10.1016/S0022-1694(02)00097-5, 2002.

Walker, G. R., Woods, P. H., and Allison, G. B.: Interlaboratory comparison of methods to determine the stable isotope composition of soil water, Chem. Geolo., 111, 297–306, doi:10.1016/0009-2541 (94) 90096-5, 1994.

Wang, B., and Gao, X.: Temporal and spatial variations of water resources constraint intensity on urbanization in the Shiyang River Basin, China, Environ. Dev.Sustain., 23(4), 1-18, doi: 10.1007/s10668-020-01045-w, 2021.

Wang, G., Xia, J., Chen, J.: Quantification of effects of climate variations and human activities on runoff by a monthly water balance model: A case study of the Chaobai River basin in northern China, Water resources research., 45(7), doi: 10.1029/2007WR006768, 2009.

Wang, T., Wang, H. S., Sun, G. W., Huang, D., and Shen, J. H.: Length-weight and length-length relationships for some Yangtze River fishes in Tian－e－zhou Oxbow, China, J. Appl. Ichthyol., 28(4), 660-662, doi:10.1111/j.1439-0426.2012.01971.x, 2012.

Wei, W., Shi, P. J., Zhou, J. J.,Feng, H. C., Wang, X. F and Wang, X. P.: Environmental suitability evaluation for human settlements in an arid inland river basin: A case study of the Shiyang River Basin, Journal of Geographical Sciences., 23(2):331-343, doi: 10.4028/www.scientific.net/AMR.518-523.4874, 2013.

West, A. G., Goldsmith, G. R., Brooks, P. D., and Dawson, T. E.: Discrepancies between isotope ratio infrared spectroscopy and isotope ratio mass spectrometry for the stable isotope analysis of plant and soil waters, Rapid. Commun. Mass. Sp., 24, 2687-2688, doi:10.1002/rcm.4685, 2010.

Worden, J., Noone, D.,and Bowman, K.: Importance of rain evaporation and continental convection in the tropical water cycle, Nature., 445(7127):528-532, doi: 10.1038/nature05508, 2007.

Salmaso, N., and Decet, F.: Seasonal and interannual changes of chemical characteristics and phytoplankton in a mountain lake of the eastern Italian Alps (Lake Calaita, Trentino), Internationale Revue der Gesamten Hydrobiologie und Hydrographie, 82(1): 15-31, doi: 10.1002/iroh.19970820104, 1997.

Zannoni, D., Steen-Larsen, H. C , Rampazzo, G., Dreossi, G., Stenni, B., and Bergamasco, A.: The atmospheric water cycle of a coastal lagoon: an isotope study of the interactions between water vapor, precipitation and surface waters, J. Hydrol., 572, 630-644, doi:10.1016/j.jhydrol.2019.03.033, 2019.

Zhang, F., Jin, G., and Liu, G.: Evaluation of virtual water trade in the yellow river delta, China, Sci. Total. Environ.,, 784, doi:10.1016/j.scitotenv.2021.147285, 2021.

Zhou, J. J., Zhao,Y. R., Huang, P., and Liu, C. F.: Impacts of ecological restoration projects on the ecosystem carbon storage of inland river basin in arid area, China, Ecol. Indic., doi:10.1016/j.ecolind.2020.106803, 2020.

Zhu, G. F. Data sets of Stable water isotope monitoring network of different water bodies in Shiyang River Basin, a typical arid river in China, Mendeley Data, V2, doi: 10.17632/vhm44t74sy.2, 2022.

Zhu, G. F., Guo, H. W., Qin, D. H., Pan, H. X, and Ma, X. G: Contribution of recycled moisture to precipitation in the monsoon marginal zone: estimate based on stable isotope data, J. Hydrol., 569, doi:10.1016/j.jhydrol.2018.12.014, 2018.

Zhu, G. F., Sang, L. Y., Zhang, Z.X., Sun, Z.G., Ma, H.Y., Liu, Y,W., Zhao, K. L., Wang, L., & Guo, H. W.: Impact of landscape dams on river water cycle in urban and peri-urban areas in the Shiyang River Basin: Evidence obtained from hydrogen and oxygen isotopes, J. Hydrol., doi:10.1016/J.JHYDROL.2021.126779, 2021a.

Zhu, G. F., Wan, Q. Z ., Yong, L. L., Li, Q. Q., Zhang, Z. Y., Guo, H. W., Zhang, Y., Sun, Z.G., Zhang, Z. X., and Ma, H. Y.: Dissolved organic carbon transport in the Qilian mountainous areas of China, Hydrol. Processes., 34, doi:10.1002/hyp.13918, 2020.

Zhu, G. F., Zhang, Z. X., Guo, H. W., Zhang, Y., Yong, L. L., Wan, Q. Z., Sun, Z. G.,and Ma, H. Y.: Below-Cloud Evaporation of Precipitation Isotopes over Mountains, Oases, and Deserts in Arid Areas. Journal of Hydrometeorology, 22(10), 2533-2545, doi: 10.1175/JHM-D-20-0170.1, 2021b.

Zhu, G. F., Yong, L. L., Zhang, Z. X., Sun, Z. G., Sang, L. L., Liu, Y., Wang, L., and Guo, H. W.: Infiltration process of irrigation water in oasis farmland and its enlightenment to optimization of irrigation mode: based on stable isotope data, Agr.Water. Manage., 258, doi: 10.1016/j.agwat.2021.107173, 2021c.

Zhu, G. F.,Yong, L. L., Zhang, Z. X., Sun, Z. G.,Wan, Q. Z., Xu, Y. X., Ma, H. Y., Sang, L. Y., Liu, Yu. W., Wang, L., Zhao, K. K., and Guo, H.W.: Effects of plastic mulch on soil water migration in arid oasis farmland: Evidence of stable isotopes, Catena., doi:10.1016/J.CATENA.2021.105580, 2021d.